

# Half-sided Translations and the Information Recovery from Radiation

Krishna Jalan, Roji Pius, Manish Ramchander

*The Institute of Mathematical Sciences, IV Cross Road, C.I.T. Campus, Taramani, Chennai, India 600113*

*Homi Bhabha National Institute, Training School Complex, Anushakti Nagar, Mumbai, India 400094*

*E-mail:* [krishnajalan@imsc.res.in](mailto:krishnajalan@imsc.res.in), [rojipius@imsc.res.in](mailto:rojipius@imsc.res.in),  
[manishd@imsc.res.in](mailto:manishd@imsc.res.in)

## Abstract

The island paradigm asserts that after the Page time the operators in the interior of an  $\text{AdS}_2$  eternal black hole in equilibrium with a finite temperature non-gravitating bath can not be reconstructed using the operators in the black hole region outside the horizon. In [1], we demonstrated this using the black hole interior reconstruction proposal due to Leutheusser and Liu, based on the half-sided translations. This was done by introducing a notion of the reduced half-sided translations associated with the algebra of operators restricted to the black hole region outside the horizon, and by showing that albeit the reduced half-sided translations translate operators in the black hole region outside the horizon to the black hole interior before the Page time, it fails to do so after the Page time. In this paper, we demonstrate the second assertion of the island paradigm, which states that after the Page time the operators in the black hole interior can be reconstructed using the operators in the bath. We show that even though before the Page time the reduced half-sided translations associated with the algebra of operators restricted to the bath do not translate operators in the bath to the black hole interior, after the Page time they take them to the black hole interior.

---

## Contents

<b>1</b>	<b>Introduction</b>	<b>1</b>
<b>2</b>	<b>The island paradigm and the reduced half-sided translations</b>	<b>3</b>
2.1	The island paradigm for a black hole in equilibrium with a bath	3
2.2	The reduced half-sided translations associated with the bath	5
<b>3</b>	<b>The reduced half-sided translations before the Page time</b>	<b>9</b>
3.1	The free energy of the trivial saddle	11
3.2	The action of the reduced half-sided translations before the Page time	12
<b>4</b>	<b>The reduced half-sided translations after the Page time</b>	<b>13</b>
4.1	The wormhole geometry	14
4.2	The wormhole saddle	15
4.3	The modular flow for a free chiral scalar in two intervals	21
4.4	The action of the reduced half-sided translations after the Page time	22
<b>5</b>	<b>Conclusion</b>	<b>23</b>

---

## 1 Introduction

One of the most significant progresses towards a consistent resolution of black hole information paradox [2–4] is the island paradigm. It posits that the black hole evaporation is a unitary evolution, and it is possible to reconstruct all the information went into the black hole using the the Hawking radiation collected at the future null infinity of the spacetime [5, 6]. The island paradigm, when it is applied to an AdS<sub>2</sub> eternal black hole in thermal equilibrium with a non-gravitating bath, asserts that before the Page time, the operators in the interior of the black hole can be reconstructed using the operators in the left and right exterior of the black hole within the gravitational region. However, after the Page time, the interior of the black hole can not be reconstructed this way. After the Page time, the interior reconstruction exclusively depends on the operators in the non-gravitating bath [7]. These assertions need to be demonstrated using a concrete black hole interior reconstruction method. There are two concrete interior reconstruction proposals. One is the Papadodimos-Raju proposal [8] and the

other is the Leutheusser-Liu proposal. In [9, 10], Leutheusser and Liu in propounded that the half-sided translations<sup>1</sup> describe the time evolution of operators, both in the exterior and in the interior of a black hole. Furthermore, it can be interpreted as a procedure for reconstructing the operators inside a black hole using the operators outside the black hole horizon.

In [1], we demonstrated the first assertion of the island paradigm using the half-sided translations. For this, we introduced the notion of reduced half-sided translations which act only on operators in the algebra of operators restricted to the black hole region outside the horizon. Then we showed that albeit the reduced half-sided translations translate operators in the black hole region outside the horizon to the black hole interior before the Page time, they fail to do so after the Page time. Let us succinctly explain the need for introducing the notion of the reduced half-sided translations. Assume that  $\mathcal{M}$  is a von Neumann algebra defined in a wedge region within the right side of the black hole inside the  $\text{AdS}_2$  boundary, and  $\mathcal{N}$  is a subalgebra of  $\mathcal{M}$ . The half-sided translation defined for this choice of algebras and an appropriate cyclic and separating state  $|\Omega\rangle$  can be constructed using the modular operators of  $\mathcal{M}$  and  $\mathcal{N}$ . However, the modular operator acts both on the operator algebra and its commutant algebra. Although,  $\mathcal{M}$  and  $\mathcal{N}$  are completely inside the gravitational region, their commutant algebras are defined in regions that also contain the bath. As a result, the half-sided translations constructed for  $\mathcal{M}$  and  $\mathcal{N}$  have non-trivial action on the operators in the bath. This implies that the interior operators reconstructed using the half-sided translations may also depend on the operators in the bath. Therefore, the reconstruction method based on the half-side translations is not convenient for illustrating the island paradigm. However, we can get around this by introducing the notion of the reduced half-sided translations. They are constructed using the reduced modular operators obtained by tracing the modular operators over  $\mathcal{H}_B$ , the GNS Hilbert space of the bath built by considering all the states obtained by acting the operators in the bath on  $|\Omega\rangle$ . Consequently, the operators in the black hole interior reconstructed using the reduced half-sided translations are expected to depend only on the operators in the gravitational region outside the horizon.

In this paper, we substantiate the second assertion of the island paradigm using the reduced half-sided translations constructed using the reduced modular operators obtained by taking the trace of the modular operators over  $\mathcal{H}_{BH}$ , the GNS Hilbert space of the black hole built by considering the set of all states obtained by acting the operators in the exterior of the black hole on  $|\Omega\rangle$ . We show that these reduced

---

<sup>1</sup>The half-sided translations are operations defined using a von Neumann operator algebra and its subalgebra. Moreover, the set of all half-sided translations form a group [11].

half-sided translations do not translate operators in the bath to the black hole interior before the Page time. Nevertheless, using the gravity path integral we argue that the action of the reduced half-sided translations alter after the Page time due to a change in the saddle. We show that the new wormhole saddle enables the reduced half-sided translations to successfully spread the operators in the bath to the black hole interior.

The organization of the paper is as follows. In section 2, we briefly discuss the island paradigm in the context of an AdS<sub>2</sub> eternal black hole in thermal equilibrium with a bath, and explain the need for introducing the notion of the reduced half-sided translations. In section 3, we delineate the JT-gravity path integral description for the reduced half-sided translations defined with respect to the bath, and show that before the Page time the reduced half-sided translations fail to translate operators in the bath to the black hole interior. In section 4, we explain how the wormhole saddle enables the reduced half-sided translations to spread an operator localised around a point in the bath to the blackhole interior. In section 5, we conclude by mentioning an interesting direction that deserves further investigation.

## 2 The island paradigm and the reduced half-sided translations

In this section, we shall briefly discuss the island paradigm in the context of AdS<sub>2</sub> eternal black hole in thermal equilibrium with a non-gravitating bath, and explain the need for introducing the notion of the reduced half-sided translations.

### 2.1 The island paradigm for a black hole in equilibrium with a bath

Consider an AdS<sub>2</sub> eternal black hole solution in JT gravity with inverse temperature  $\beta$  coupled to a non-gravitating bath having the same inverse temperature. The matter in the spacetime is chosen to be a CFT having central charge  $c$ . To make the computations manageable, we assume that the matter CFT is not directly coupled to the dilaton. The thermal equilibrium guarantees that the classical geometry of the black hole spacetime is the same as that of an isolated eternal black hole. The coupled system can be conveniently described as a region in a plane with the Kruskal coordinates  $(w^+, w^-)$  [7], see figure 1. The AdS<sub>2</sub> black hole region (the gravitational region) in the  $w$ -plane is given by the equation

$$w^+ w^- \geq -e^{\frac{4\pi\epsilon}{\beta}}, \quad (2.1)$$

where  $\epsilon$  is a real parameter that specifies the location of the cut-out boundary of AdS<sub>2</sub>. The bath is the remaining region in the  $w$ -plane. The black hole horizon is given by

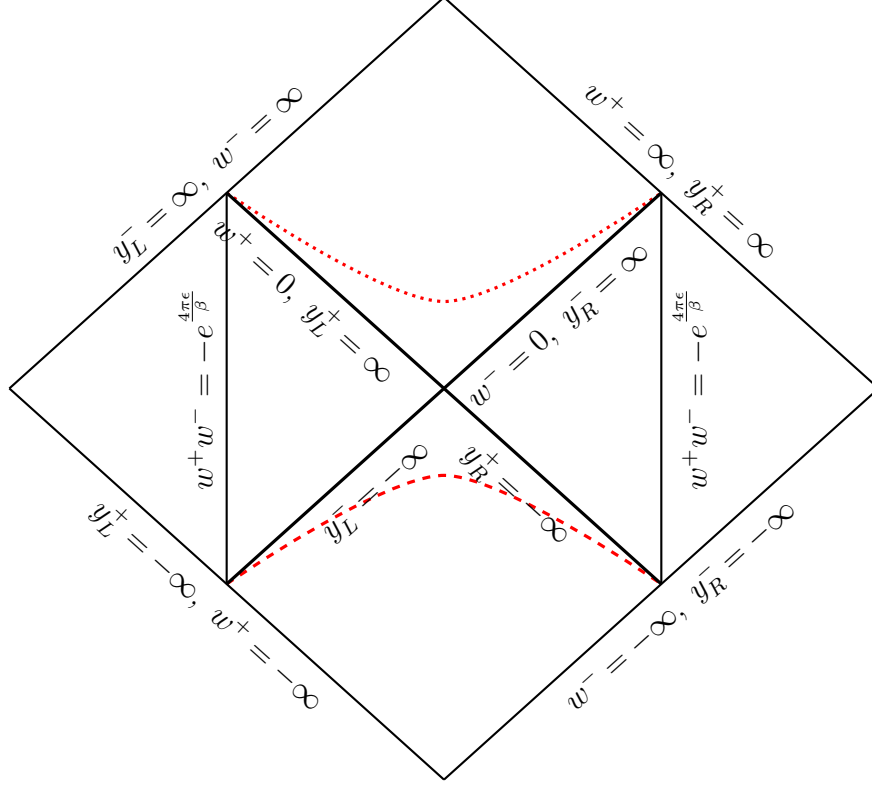


**Figure 1.** An eternal black hole in equilibrium with a finite temperature bath can be described using a plane with light cone coordinates  $(w^+, w^-)$ . The right/left Rindler wedge describes the right/left side of the black exterior coupled to the right/left bath having flat metric. The right/left Rindler wedge can be covered using the light cone coordinates  $(y_{R/L}^+, y_{R/L}^-)$ . The lines  $w^+ w^- = 0$  are the future and the past horizons of the eternal black hole. The interface between the black hole and the bath satisfy the equation  $w^+ w^- = -e^{\frac{4\pi\epsilon}{\beta}}$ . The red dashed hyperbola represents the singularity on which the dilaton profile vanishes.

the equation  $w^+ w^- = 0$ , and the past and the future singularities of the black hole lie on the hyperbolas on which the following dilaton profile vanish

$$\phi(w^+, w^-) = \phi_0 + \frac{2\pi\phi_r}{\beta} \frac{1 - w^+ w^-}{1 + w^+ w^-}, \quad (2.2)$$

where the first term  $\phi_0$  give rises to the extremal entropy, and  $\frac{\phi_r}{\epsilon}$  is the boundary value of the difference  $\phi(w^+, w^-) - \phi_0$ . The right and left exteriors of the black hole can be covered with the Minkowski coordinates  $(y_R^+, y_R^-)$  and  $(y_L^+, y_L^-)$  in the left and the right bath respectively. They are related to the  $(w^+, w^-)$  coordinates as follows

$$w^\pm = \pm e^{\pm \frac{2\pi y_R^\pm}{\beta}}, \quad w^\pm = \mp e^{\mp \frac{2\pi y_L^\pm}{\beta}}. \quad (2.3)$$

In this coordinate system, the metric in the AdS<sub>2</sub> region is given by

$$ds_{BH}^2 = \frac{4dw^+dw^-}{(1+w^+w^-)^2}, \quad (2.4)$$

and the metric in the bath region is given by

$$ds_B^2 = \frac{\beta^2}{4\pi^2\epsilon^2} \frac{dw^+dw^-}{w^+w^-}. \quad (2.5)$$

Although the geometry of an AdS<sub>2</sub> eternal black hole in equilibrium with a thermal bath is the same as that of an AdS<sub>2</sub> eternal black hole with reflecting boundary conditions at the boundary, quantum mechanically the two systems have drastic differences. The constant exchange of matter between the black hole and the bath give rises to an ever-growing entanglement between them. This can be seen by computing the entanglement entropy of the bath. In fact, a short computation of the bath entropy using the replica method [12] reveals that at late times the entanglement entropy of both the black hole and the bath rises linearly with respect to the boundary time  $u$

$$S_{\text{blackhole}}(u) = S_{\text{bath}}(u) \xrightarrow{u \gg \beta} \frac{2\pi c}{3\beta} u. \quad (2.6)$$

The linear growth makes the von-Neumann entanglement entropy bigger than the thermal entropy of the black hole at sufficiently large times. The paradoxical growth of the von Neumann entropy can be resolved by changing the saddle of the gravitational replica path integral from the trivial saddle to the saddle having minimum free energy. After the Page time the saddle having the least free energy is a Euclidean wormhole geometry [7, 13]. The replica wormhole introduces a non-trivial entanglement wedge island, containing the black hole interior, for the bath. The inclusion of this island into the entropy computation of the bath tame the linear growth of bath entropy and makes it a constant equal to the thermal entropy of the black hole. The consistency of this paradigm require that after the Page time the degrees of freedom inside the black hole is not reconstructable using the degrees of freedom outside the horizon restricted to the gravitational region, i.e. inside the left and the right cut-out AdS<sub>2</sub> boundaries. Nevertheless, it must be possible to reconstruct the degrees of freedom inside the black hole interior using only the degrees of freedom in the bath region after the Page time.

## 2.2 The reduced half-sided translations associated with the bath

The half-sided translations are operations performed on a von-Neumann algebra that form a continuous one-parametric unitary group. The unitary group is defined with respect to a von Neumann algebra  $\mathcal{M}$ , with a cyclic and separating vector  $|\Omega\rangle$ , and

a subalgebra  $\mathcal{N}$  with the same cyclic and separating vector. The separating property of  $|\Omega\rangle$  implies that it is not annihilated by any of the operators in  $\mathcal{M}$ . The cyclic property of  $|\Omega\rangle$  means that a dense subspace of the Hilbert space associated with  $\mathcal{M}$  can be obtained by acting with the elements of  $\mathcal{M}$  on  $|\Omega\rangle$ . An element of this group is given by

$$U(s) = \Delta_{\mathcal{M}}^{-it} \Delta_{\mathcal{N}}^{it}, \quad s = e^{-2\pi t} - 1 \quad \forall t \leq 0. \quad (2.7)$$

where  $\Delta_{\mathcal{M}}$  and  $\Delta_{\mathcal{N}}$  are the modular operators associated with the algebras  $\mathcal{M}$  and  $\mathcal{N}$  respectively [11]. The modular operator  $\Delta_{\mathcal{M}}$  can be determined using the Tomita operator  $S_{\mathcal{M}}$  for  $|\Omega\rangle$ . It is defined by

$$S_{\mathcal{M}} a |\Omega\rangle = a^\dagger |\Omega\rangle, \quad (2.8)$$

for all  $a \in \mathcal{M}$ . Since the Tomita operator is invertible, it has a unique polar decomposition into a product of antiunitary operator  $J_{\mathcal{M}}$  and a hermitian and positive-definite operator  $\Delta_{\mathcal{M}}^{\frac{1}{2}}$

$$S_{\mathcal{M}} = J_{\mathcal{M}} \Delta_{\mathcal{M}}^{\frac{1}{2}}. \quad (2.9)$$

The definition (2.8) implies that if  $\mathcal{M}$  is an operator algebra defined inside a wedge, then it can be expressed as follows

$$\Delta_{\mathcal{M}} = \rho_{\mathcal{M}'}^{-1} \otimes \rho_{\mathcal{M}}. \quad (2.10)$$

where  $\rho_{\mathcal{M}}$  is the reduced density matrix of the wedge region in which  $\mathcal{M}$  is defined and  $\rho_{\mathcal{M}'}$  is the reduced density matrix of the causally disconnected wedge region in which the commutant<sup>2</sup>  $\mathcal{M}'$  is defined [14]. Substituting (2.10) in (2.7) gives the following expression for the half-sided translations

$$U(s) = \rho_{\mathcal{M}'}^{it} \rho_{\mathcal{N}'}^{-it} \otimes \rho_{\mathcal{M}}^{-it} \rho_{\mathcal{N}}^{it} \quad s = e^{-2\pi t} - 1 \quad \forall t \leq 0. \quad (2.11)$$

Analytically continuing  $t$  to  $-i\theta$ , for  $\theta \in \mathbb{R}$  gives the following expression for the half-sided translation

$$U(s) = \rho_{\mathcal{M}'}^{\theta} \rho_{\mathcal{N}'}^{-\theta} \otimes \rho_{\mathcal{M}}^{-\theta} \rho_{\mathcal{N}}^{\theta} \quad s = e^{2\pi i\theta} - 1 \quad \forall t \leq 0. \quad (2.12)$$

The advantage of this expression is that by choosing an arbitrary integer value  $n$  for  $\theta$ , we can convert an insertion of  $U(s)$  in a correlation function into a corresponding path integral, and at the end of the manipulations,  $n$  can be continued to a real number. This is very similar to the replica trick used for computing the  $n^{\text{th}}$  Rényi entropy.

---

<sup>2</sup>Commutant  $\mathcal{M}'$  is the set of all observables that commute with all the elements in  $\mathcal{M}$

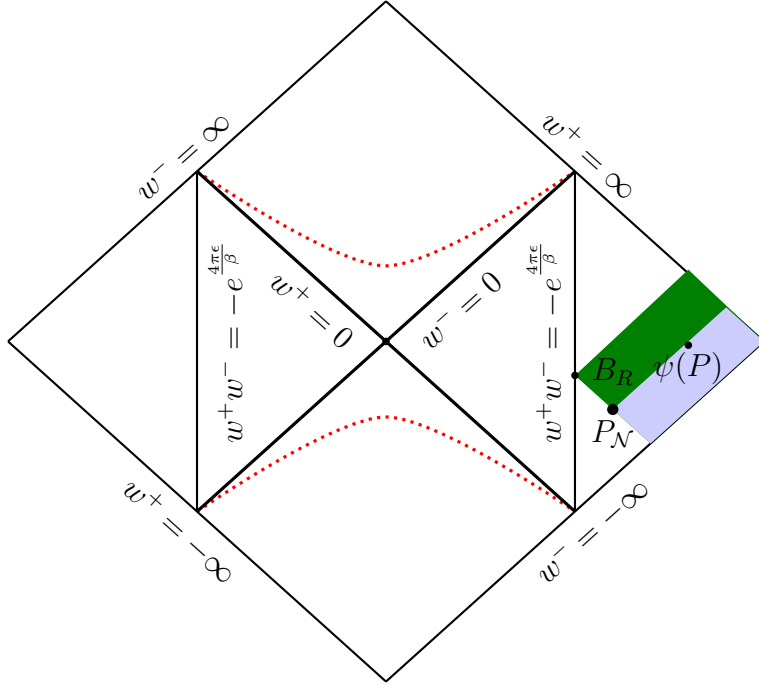


**Figure 2.** The half-sided translations are defined using the von Neumann algebra  $\mathcal{M}$  restricted to the union of the green shaded and the blue shaded wedges in the right bath and the subalgebra  $\mathcal{N}$  restricted to the blue shaded wedge.

A convenient choice of operator algebras  $\mathcal{M}$  and  $\mathcal{N}$  for defining the half-sided translation is shown in figure 2. The operator algebra defined in the union of the green shaded and the blue shaded wedges is the chosen  $\mathcal{M}$ , and  $\mathcal{N}$  is the operator algebra defined in the blue shaded region. A cyclic and separating vector can be obtained by performing the JT gravity coupled to the CFT path integral over the lower half of the  $w$ -plane. However, the commutants of  $\mathcal{M}'$  and  $\mathcal{N}'$  are wedge algebras that extend also to the  $\text{AdS}_2$  black hole region, see figure 3. Therefore, an operator in the black hole interior reconstructed via the half-sided translations defined using  $\mathcal{M}$  and  $\mathcal{N}$  can not be expressed only in terms of the operators in the bath. To get around this, following [1] we shall use the notion of the reduced half-sided translations which at the end of the construction only depend on the algebra of observables in the bath. For this, let us define the reduced modular operator  $\Delta_{\mathcal{M}}^B$  by tracing  $\Delta_{\mathcal{M}}$  over the black hole Hilbert space  $\mathcal{H}_{BH}$

$$\Delta_{\mathcal{M}}^B = \text{Tr}_{\mathcal{H}_{BH}} \Delta_{\mathcal{M}}. \quad (2.13)$$

The black hole Hilbert space  $\mathcal{H}_{BH}$  is defined as the GNS-Hilbert space [11] con-

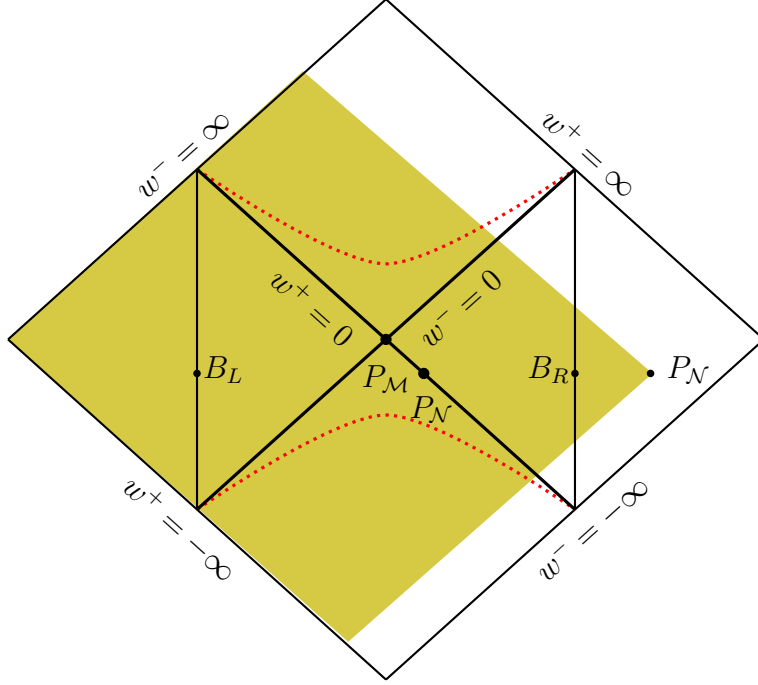


**Figure 3.** The commutant  $\mathcal{N}'$  of the von Neumann algebra  $\mathcal{MN}$  is given by the algebra of observables defined in the union of the yellow shaded wedge.

structed by considering the collection of all states obtained by the action of operators in the domain of dependence of the part of the Cauchy slice within the  $\text{AdS}_2$  black hole region on the cyclic and separating state  $|\Omega\rangle$ . The modular operator  $\Delta_{\mathcal{M}}^B$  can be understood as the modular operator defined using  $\mathcal{M}$  and the relative commutant  $\mathcal{M}'^B$  of the algebra  $\mathcal{M}$  within the operator algebra defined in the bath region, see figure 4. The relative modular operator  $\Delta_{\mathcal{M}}^B$  can be expressed as

$$\Delta_{\mathcal{M}}^B = \rho_{\mathcal{M}'}^B{}^{-1} \otimes \rho_{\mathcal{M}}.$$

The density matrix  $\rho_{\mathcal{M}}$  is obtained by performing the JT gravity coupled to CFT path integral over the complex  $w$ -plane with a cut connecting the points  $B_R$  and  $-\infty$ . The density matrix  $\rho_{\mathcal{M}'}^B$  is obtained by performing the path integral over the same complex plane with a cut connecting the points  $B_L$  and  $-\infty$ . Similarly, the relative modular operator  $\Delta_{\mathcal{N}}^B$  can be expressed as

$$\Delta_{\mathcal{N}}^B = \rho_{\mathcal{N}'}^B{}^{-1} \otimes \rho_{\mathcal{N}}.$$

The density matrix  $\rho_{\mathcal{N}}$  is obtained by performing the path integral over the  $w$ -plane with a cut connecting the points  $P_{\mathcal{N}}$  and  $\infty$ . The density matrix  $\rho_{\mathcal{M}'}^B$  is obtained by

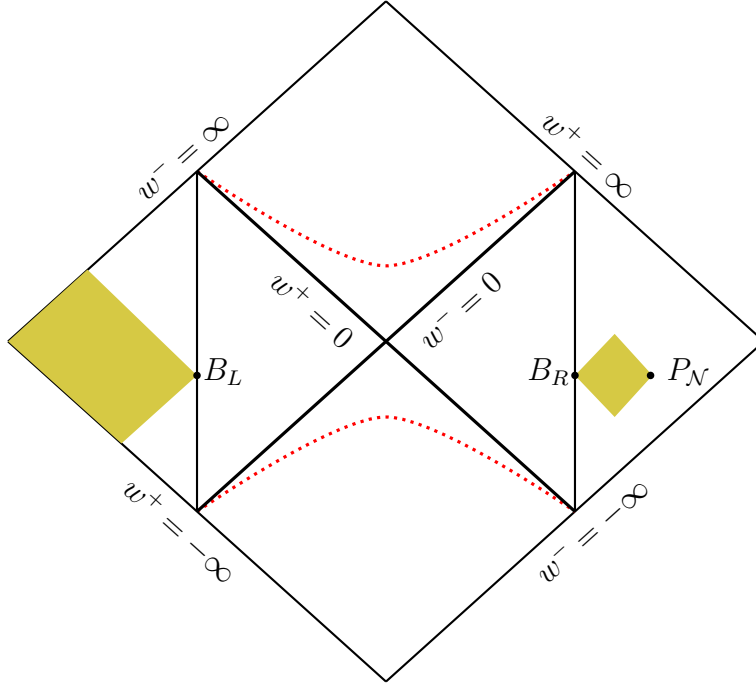


**Figure 4.** The relative commutant  $\mathcal{N}^B$  of the von Neumann algebra  $\mathcal{N}$  within the bath region is given by algebra of observables defined in the two yellow shaded wedge.

performing the path integral over the same  $w$ - plane with two cuts, one cut connecting the points  $B_R$  and  $P_N$ , and the other cut connecting the points  $B_L$  and  $-\infty$ . Using these reduced modular operators  $\Delta_{\mathcal{M}}^B$  and  $\Delta_{\mathcal{N}}^B$  we can define the reduced half-sided translation  $U^B(s)$  as given below

$$U^B(s) = (\Delta_{\mathcal{M}}^B)^{-it} (\Delta_{\mathcal{N}}^B)^{it}. \quad (2.14)$$

### 3 The reduced half-sided translations before the Page time

In this section, we shall identify the generator of the half sided translations before the Page time by analysing the action of  $U^B(s)$ , for infinitesimal values of  $s$ , on a local operator  $\psi$  of the matter CFT placed at a point  $P$  in the bath attached to the right side of the  $\text{AdS}_2$  black hole, see figure 2. The action of the half-sided translations  $U^B(s)$  on the local operator can be investigated using the path integral description of the action of half-sided translations on a local operator inserted in an arbitrary correlation function

$$\langle \Omega | \cdots (U^B(s))^\dagger \psi(w_P^+, w_P^-) U^B(s) \cdots | \Omega \rangle$$

as discussed in [15]. The dots represent all the other local operator insertions away from the point  $P$  where the operator  $\psi$  is inserted. Using the expression for  $U^B(s)$  in terms of the modular operators, we can write down the Euclidean continuation of this correlation function as follows

$$\begin{aligned} & \langle \Omega | \cdots U^B(-s) \psi(w_P, \bar{w}_P) U^B(s) \cdots | \Omega \rangle \\ &= \langle \Omega | \cdots (\Delta_{\mathcal{N}}^B)^{-\theta} (\Delta_{\mathcal{M}}^B)^\theta \psi(w_P, \bar{w}_P) (\Delta_{\mathcal{M}}^B)^{-\theta} (\Delta_{\mathcal{N}}^B)^\theta \cdots | \Omega \rangle \end{aligned} \quad (3.1)$$

where  $\theta = -\frac{i}{2\pi} \ln(1+s)$ . Initially, we assume  $\theta$  to be an integer  $n$ , and at the end of the manipulation we analytically continue  $n$  back to an infinitesimal real number, since our main aim is to find the generator of the reduced half-sided translations.

The path integral representation of the modular operator  $\Delta_{\mathcal{M}}^B$  is given by the JT-gravity path integral over a pair of  $w$ -planes identified at the point  $P_{\mathcal{M}}$ , each with a cut. The cut in one of the  $w$ -plane connects the points  $B_R$  and  $\infty$  and the cut in the second plane connects the points  $B_L$  and  $-\infty$ . Likewise, the modular operator  $\Delta_{\mathcal{N}}^B$  is given by the path integral over two  $w$ -planes identified at the point  $P_{\mathcal{N}}$ , each with cuts. One of the  $w$ -plane has a cut connecting the points  $P_{\mathcal{N}}$  and  $\infty$ , and the second plane has two cuts, one cut connects the point  $P_{\mathcal{N}}$  and  $B_R$  and the second cut connects  $B_L$  and  $-\infty$ . The points  $B_R$  and  $B_L$  in the Euclidean  $w$ -plane, after the analytic continuation of the Euclidean time to Lorentzian time  $\tau \rightarrow \tau + iu$ , correspond to the points in the Lorentzian  $w$ -plane where the equal time slice  $\Sigma_u$ , parameterised by the AdS<sub>2</sub> boundary time  $u$ , intersects with the right and the left cut-out AdS<sub>2</sub> boundaries respectively. The Lorentzian coordinates of the points  $B_L$  and  $B_R$  at boundary time  $u$  are given by

$$\begin{aligned} (w_{B_L}^+, w_{B_L}^-) &= \left( -e^{-\frac{2\pi(u-\epsilon)}{\beta}}, e^{\frac{2\pi(u+\epsilon)}{\beta}} \right), \\ (w_{B_R}^+, w_{B_R}^-) &= \left( e^{\frac{2\pi(u-\epsilon)}{\beta}}, -e^{-\frac{2\pi(u+\epsilon)}{\beta}} \right) \end{aligned} \quad (3.2)$$

Then the path integral description of

$$\langle \Omega | \cdots (\Delta_{\mathcal{N}}^B)^{-n} (\Delta_{\mathcal{M}}^B)^n \psi(w_P, \bar{w}_P) (\Delta_{\mathcal{M}}^B)^{-n} (\Delta_{\mathcal{N}}^B)^n \cdots | \Omega \rangle$$

is obtained by gluing the  $4n$  pair of  $w$ -planes representing the modular operators and the  $w$ -plane where the operator  $\psi(P)$  is inserted along the cuts. Since the path integral involves JT gravity, we must consider the sum over all possible geometries that respect the sewing along the cuts in the bath and also consistent with the JT gravity constraints [16]. Finally, the action of the half-sided translation can be found by determining the JT gravity path integral saddle with the least free energy.

The dominant saddle before the Page time is the trivial saddle. It can be constructed by sewing the  $8n+1$  number of  $w$ -planes along various cuts as described in

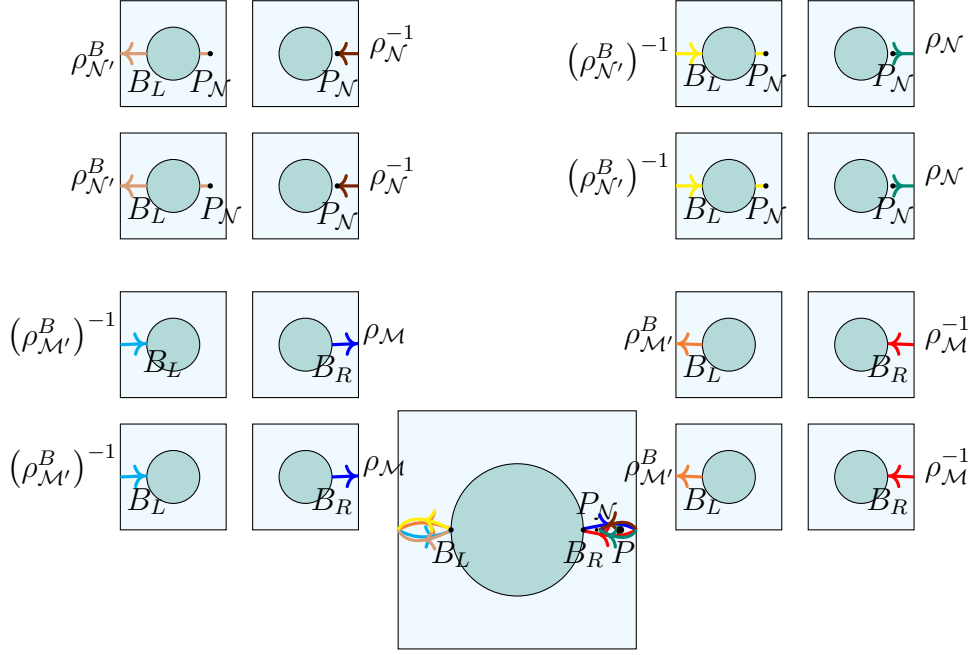


**Figure 5.** The trivial saddle is obtained by cyclically gluing the  $w$ -planes along the cuts having same colours. The resulting Riemann surface viewed as a sheeted geometry over the  $w$ -plane has branch points at locations  $B_L, B_R$  and  $P_N$  on the  $w$ -plane. The figure describes the gluing for  $n = 2$ .

figure 5. In which,  $8n$  number of  $w$ -planes represent the density matrices appearing in  $U^B(s)$  and  $(U^B(s))^\dagger$ . The local operator  $\psi$  is inserted in the remaining  $w$ -plane. The resulting Riemann surface has eight conical singularities at points  $B_R$  and  $B_L$  on the  $w$ -plane.

### 3.1 The free energy of the trivial saddle

Let us compute the leading term in the free energy of the trivial saddle at large boundary time  $u$ . This saddle is a sheeted geometry with various conical singularities. In such cases, usually the leading contributions to the free energy of the saddle come from the conical singularities. For a CFT having central charge  $c$  sheeted geometry, the contribution to the free energy from a conical singularity with excess angle  $\gamma$  is given by [17]

$$\Delta F \approx \frac{c(\gamma + 2\pi)}{24\pi} \left( 1 - \left( \frac{2\pi}{(\gamma + 2\pi)} \right)^2 \right) \ln L, \quad (3.3)$$

where  $L$  is the radius of the largest disk around the conical singularity that does not include any other conical singularities. In our problem, the conical singularities are at

$B_R$  and  $B_L$ , and the length  $L$  is given by

$$L = \sqrt{(w_{B_R} - w_{B_L})(\bar{w}_{B_R} - \bar{w}_{B_L})}. \quad (3.4)$$

Hence, the free energy of the trivial saddle at time  $u$  is obtained by summing over all the contributions from the conical singularities followed by the Lorentzian continuation, and is given by

$$F_T \approx \frac{2(n+1)c}{3} \left(1 - \frac{1}{(n+1)^2}\right) \ln \left(\frac{\beta}{\pi\epsilon} \cosh \left(\frac{2\pi u}{\beta}\right)\right). \quad (3.5)$$

For large  $u$ ,  $F_T$  can be approximated as follows

$$\mathcal{F}_T(u) \approx \frac{4\pi(n+1)c}{3\beta} \left(1 - \frac{1}{(n+1)^2}\right) u. \quad (3.6)$$

### 3.2 The action of the reduced half-sided translations before the Page time

The action of half-sided translation can be studied using  $\mathcal{K}_{\mathcal{M}}$  and  $\mathcal{K}_{\mathcal{N}}$ , the modular Hamiltonians associated with the operator algebras  $\mathcal{M}$  and  $\mathcal{N}$  respectively. Interestingly, for a CFT the modular Hamiltonian of a wedge region generates the flow of the conformal boost Killing vector [18]. Therefore, the modular Hamiltonians  $\mathcal{K}_{\mathcal{M}}$  and  $\mathcal{K}_{\mathcal{N}}$  can be constructed using the conformal boost Killing vectors  $\zeta_{\mathcal{M}}$  and  $\zeta_{\mathcal{N}}$  associated with the wedge regions where the algebras  $\mathcal{M}$  and  $\mathcal{N}$  are defined

$$\mathcal{K}_{\mathcal{M}} = \int_{\Sigma_{\mathcal{M}}} T_{ab} \zeta_{\mathcal{M}}^a d\Sigma_{\mathcal{M}}^b + \int_{\Sigma_{\mathcal{M}'}} T_{ab} \zeta_{\mathcal{M}'}^a d\Sigma_{\mathcal{M}'}^b, \quad (3.7)$$

$$\mathcal{K}_{\mathcal{N}} = \int_{\Sigma_{\mathcal{N}}} T_{ab} \zeta_{\mathcal{N}}^a d\Sigma_{\mathcal{N}}^b + \int_{\Sigma_{\mathcal{N}'}} T_{ab} \zeta_{\mathcal{N}'}^a d\Sigma_{\mathcal{N}'}^b, \quad (3.8)$$

where  $T_{ab}$  is the component of the CFT stress tensor,  $\Sigma_{\mathcal{W}}$  is the part of the Cauchy slice in the  $w$ -plane that is within the wedges region associated with algebra  $\mathcal{W}$ , for  $\mathcal{W} = \mathcal{M}, \mathcal{N}, \mathcal{M}'$  and  $\mathcal{N}'$ . Using  $\mathcal{K}_{\mathcal{M}}$  and  $\mathcal{K}_{\mathcal{N}}$ , the generator of the half-sided translations can be constructed [11], and is given by

$$G = \frac{1}{2\pi} (\mathcal{K}_{\mathcal{M}} - \mathcal{K}_{\mathcal{N}}) = \frac{1}{2\pi} \int_{\Sigma_{\mathcal{N}}} T_{ab} (\zeta_{\mathcal{M}}^a - \zeta_{\mathcal{N}}^a) d\Sigma_{\mathcal{M}}^b + \frac{1}{2\pi} \int_{\Sigma_{\mathcal{M}} - \Sigma_{\mathcal{N}}} T_{ab} (\zeta_{\mathcal{M}}^a - \zeta_{\mathcal{N}'}^a) d\Sigma_{\mathcal{M}}^b. \quad (3.9)$$

Since we have traced over the AdS<sub>2</sub> black hole region, and  $\mathcal{M}$  is the full domain of dependence of the Cauchy slice within the right bath we must choose only those conformal boost killing vectors  $\zeta_{\mathcal{M}}$  and  $\zeta_{\mathcal{N}}$  that vanish at the boundary of the wedge region where algebra  $\mathcal{M}$  is defined. This implies that the action of  $G$  vanishes at the boundary of this wedge. Consequently, the half-sided translation can not translate a local operator outside this wedge region. Hence, we conclude that before the Page time the reduced half-sided translations associated with the bath can not reconstruct operators in the interior of the black hole.

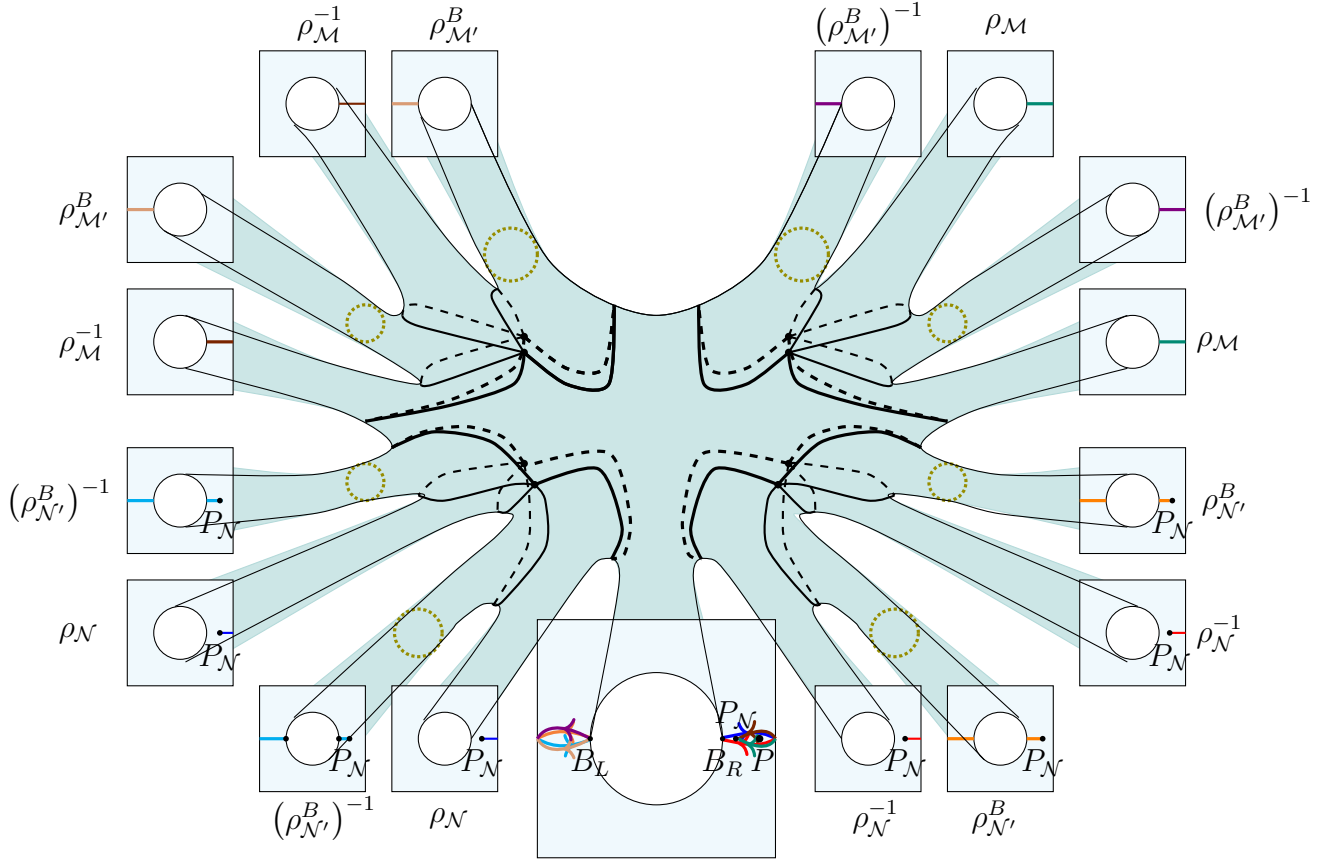


**Figure 6.** A wormhole geometry with  $8n + 1$  number of boundaries with copies of bath attached to each of them. It has a smooth hyperbolic metric in the gravitational region, without any conical singularities. The thick coloured lines indicate cuts. All the cuts with the same colour are being cyclicly glued. Slicing the geometry along the black curves on it produces  $8n + 1$  component surfaces. In which  $4n$  number of component surfaces have the geometry of a  $w$ -plane with a cut in the gravitational region and a cut in the non-gravitating bath.  $4n$  number of component surfaces have the geometry of a  $w$ -plane with one cut in the gravitational region and two cuts in the bath. The remaining one piece has the geometry of a  $w$ -plane with four cuts in the gravitational region and eight closely placed cuts in the bath. In this figure,  $n$  is chosen to be 2.

#### 4 The reduced half-sided translations after the Page time

In this section, we shall study the action of the half-sided translation after the Page time. We do this by constructing a wormhole geometry that satisfies the JT gravity constraint and contributes to the path integral representation of

$$\langle \Omega | (\rho_{N'}^B)^n \otimes \rho_{N'}^{-n} (\rho_{M'}^B)^{-n} \otimes \rho_M^n \psi(w_P, \bar{w}_P) \rho_M^{-n} \otimes (\rho_{M'}^B)^n \rho_{N'}^n \otimes (\rho_{N'}^B)^{-n} | \Omega \rangle.$$

Unlike the trivial saddles, a non-trivial saddle has bridges connecting different  $w$ -planes that are being glued along the cuts in the non-gravitating bath region. Since the matter CFT is not coupled to the JT gravity dilaton, the constraint demands that the wormhole must have curvature  $R = -2$ , i.e. the wormhole must be a hyperbolic Riemann surface. We will construct such a wormhole by identifying the geodesic edges of a set of hyperbolic quadrilaterals. We shall then identify the wormhole saddle by minimising the free energy of the wormhole geometry. The minimisation of free energy will allow us to identify the value of the moduli parameters of the wormhole geometry that corresponds to the wormhole saddle.

#### 4.1 The wormhole geometry

Our strategy to identify the wormhole saddle is the following. First construct a wormhole geometry with hyperbolic metric by gluing a set of hyperbolic quadrilaterals having arbitrary angles at the vertices [19, 20]. The resulting Riemann surface can have conical singularities at the points where the vertices of the hyperbolic quadrilaterals meet. We then determine the angles at the vertices of the quadrilaterals by demanding that the wormhole geometry has no conical singularities on it.

Consider the wormhole geometry described in figure 6. The gravitational region of this geometry has the topology of a sphere with  $8n + 1$  number of boundaries. All the boundaries of the gravitational region are attached to a copy of the bath. The coloured lines in the bath are cuts. The cuts in the bath having the same colour are being cyclicly glued. A hyperbolic quadrilateral decomposition of the gravitational region of this geometry can be seen by slitting the wormhole surface along the black curves. The slitting gives  $8n + 1$  number of component surfaces,  $8n$  hyperbolic disks with two cuts and a hyperbolic disk with four cuts. Interestingly, a hyperbolic disk with a cut connecting two conical singularities with angles  $2\alpha$  and  $2\beta$  can be obtained by identifying the edges of a pair of hyperbolic quadrilaterals as shown in figure 7. The edges  $P'R'$  and  $P''R''$  and the edges  $Q'S'$  and  $Q''S''$  are being identified to obtain the disk with a cut. The angles at the vertices  $R'$  and  $R''$  of the quadrilateral are  $\alpha$  and the angle at the vertices  $S'$  and  $S''$  are  $\beta$ . The boundaries of the cut that connects the conical singularities are the edges of the quadrilaterals  $S'R'$  and  $S''R''$ . Similarly, a hyperbolic disk with four cuts can be obtained by gluing fourteen hyperbolic quadrilaterals as shown in figure 8. Therefore, the gravitational region of the wormhole geometry described in figure 6 can be obtained by gluing  $16n + 14$  number of hyperbolic quadrilaterals along their geodesic boundaries.

The angles at the vertices of the hyperbolic quadrilaterals can be found by demanding that the locations on the wormhole at which the vertices of the quadrilaterals meet must not have conical deficit or excess angle. This condition is fulfilled if the angle at

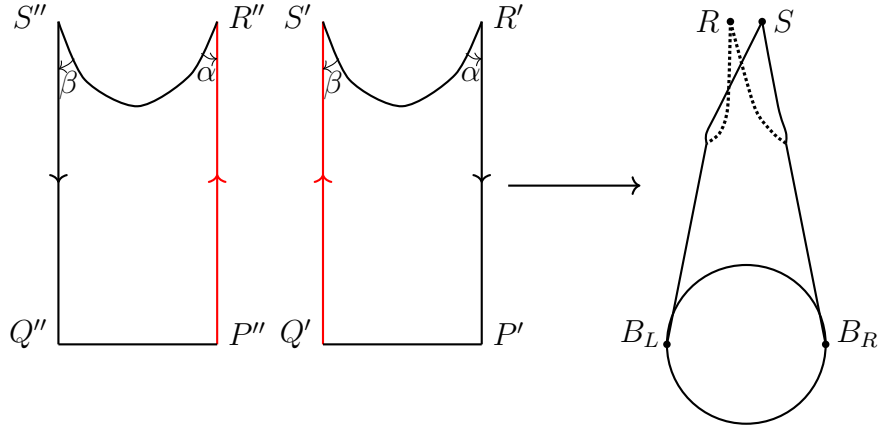


**Figure 7.** The gravitational region of the wormhole geometry can be cut into  $8n + 1$  number of pieces. In which  $8n$  pieces have the geometry of a hyperbolic disk with a cut connecting two conical singularities, one at point  $R$  and another at point  $S$ . The conical singularity at  $R$  has opening angle  $2\alpha$  and the conical singularity at  $S$  has opening angle  $2\beta$ . This geometry can be obtained by identifying the edges  $P'R'$  and  $P''R''$  and edges  $Q'S'$  and  $Q''S''$  of a pair of hyperbolic quadrilaterals. The angle at the vertices  $R'$  and  $R''$  are  $\alpha$  and the angle at the vertices  $S'$  and  $S''$  are  $\beta$ .

the vertices of a quadrilateral which meet the vertices of other  $4n + 1$  quadrilaterals is  $\frac{\pi}{2n+1}$ . This implies that the angles at the locations  $R$  and  $S$  in figure 7 are same, and is given by  $\frac{2\pi}{2n+1}$ , i.e.

$$\alpha = \beta = \frac{\pi}{2n + 1}.$$

Likewise, the angles at the locations  $Q_{N'}, Q_N, \tilde{Q}'_{N'}, \tilde{Q}_N, Q_{M'}, Q_M, \tilde{Q}'_{M'},$  and  $\tilde{Q}_M$  in figure 8 are all the same. and is given by  $\frac{2\pi}{2n+1}$ .

## 4.2 The wormhole saddle

In order to identify the wormhole saddle, we must compute the free energy of the wormhole geometry constructed using the hyperbolic quadrilaterals, and then minimise the free energy. The minimisation will determine the moduli parameters of the hyperbolic Riemann surface that describe the gravitational region of the wormhole saddle. For this, let us slit the wormhole geometry along the black curves shown in figure 6. We shall denote the resulting surface as  $\mathcal{S}$ . This surface is obtained by gluing  $8n + 1$  number of  $w$ -planes along the cuts in the bath region. These  $w$ -planes can be classified into nine groups, 8 groups containing  $n$  number of  $w$ -planes and one containing only one  $w$ -plane where the local operator  $\psi$  is inserted. They can be characterised as follows.

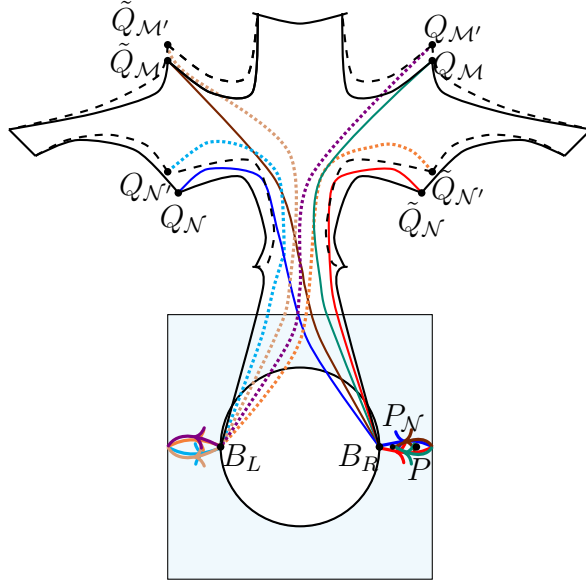


**Figure 8.** One of the piece obtained by dividing the gravitational region of the wormhole geometry into  $8n + 1$  number of pieces has the geometry of a hyperbolic disk with four cuts. The four cuts are along the curves  $Q_{N'}Q_N$ ,  $\tilde{Q}'_{N'}\tilde{Q}_N$ ,  $Q_{M'}Q_M$  and  $\tilde{Q}'_{M'}\tilde{Q}_M$ . Scissoring the surface along the coloured thick and dotted lines produces two hyperbolic quadrilaterals and three hyperbolic hexagons with two cusps. A hexagon can be further divided into four hyperbolic quadrilaterals. As a result, the surface can be constructed by identifying the edges of fourteen hyperbolic quadrilaterals.

- The first group contains  $n$  number of  $w$ -planes having one cut in their gravitational region and one cut in the bath region. The cut in the bath region begins at  $P_N$  and ends at  $+\infty$ , and the cut in the gravitational region is assumed to be connecting the conical singularities denoted as  $P_1$  and  $P'_1$ .
- The second group is similar to the first group except in the orientation of the cuts which are opposite for the elements in the first and second groups. Also the cut in the gravitational region is assumed to be connecting the conical singularities denoted as  $\tilde{P}_1$  and  $\tilde{P}'_1$ .
- The third group contains  $n$  number of  $w$ -planes having one cut in their gravitational region and one cut in the bath region. The cut in the bath region begins at  $B_R$  and ends at  $+\infty$ , and the cut in the gravitational region is assumed to be connecting the conical singularities denoted as  $P_2$  and  $P'_2$ .
- The fourth group is similar to the third group except in the orientation of the cuts which are opposite for the elements in the fourth and third groups. Also the cut

in the gravitational region is assumed to be connecting the conical singularities denoted as  $\tilde{P}_2$  and  $\tilde{P}'_2$ .

- The fifth group contains  $n$  number of  $w$ -planes having one cut in their gravitational region and two cuts in the bath region. One cut in the bath region begins at  $B_R$  and ends at  $P_{\mathcal{N}}$ , and the second cut in the bath region begins at  $-\infty$  and ends at  $B_L$ . The cut in the gravitational region is assumed to be connecting the conical singularities denoted as  $P_3$  and  $P'_3$ .
- The sixth group is similar to the fifth group except in the orientation of the cuts which are opposite for the elements in the sixth and fifth groups. Also the cut in the gravitational region is assumed to be connecting the conical singularities denoted as  $\tilde{P}_3$  and  $\tilde{P}'_3$ .
- The seventh group contains  $n$  number of  $w$ -planes having one cut in their gravitational region and one cut in the bath region. The cut in the bath region begins at  $-\infty$  and ends at  $B_L$ . The cut in the gravitational region is assumed to be connecting the conical singularities denoted as  $P_4$  and  $P'_4$ .
- The eighth group is similar to the seventh group except in the orientation of the cuts which are opposite for the elements in the eighth and seventh groups. Also the cut in the gravitational region is assumed to be connecting the conical singularities denoted as  $\tilde{P}_4$  and  $\tilde{P}'_4$ .
- The ninth group has only one  $w$ -plane in which the operator  $\psi(P)$  is inserted. It has four cuts in the gravitational region and ten closely placed cuts in the bath region. The first cut in the gravitational region connects the conical singularities  $Q_{\mathcal{N}}$  and  $Q_{\mathcal{N}'}$ , the second cut connects the conical singularities  $\tilde{Q}_{\mathcal{N}}$  and  $\tilde{Q}_{\mathcal{N}'}$ , the third cut connects the conical singularities  $Q_{\mathcal{M}}$  and  $Q_{\mathcal{M}'}$  and the fourth cut connects the conical singularities  $\tilde{Q}_{\mathcal{M}}$  and  $\tilde{Q}_{\mathcal{M}'}$ .

The identifications along the boundaries of the surface  $\mathcal{S}$  that give back the original wormhole geometry form a Fuchsian group  $\Gamma$ [19]. Therefore, the free energy of the wormhole  $F_W$  can be computed by first evaluating the free energy  $\mathcal{F}_{\mathcal{S}}$  for  $\mathcal{S}$ , followed by a summation over all the images  $\mathcal{F}_{\gamma\mathcal{S}}$  of the result under the action of all Fuchsian transformations  $\gamma$ , i.e.

$$F_W = \sum_{\gamma \in \Gamma} \mathcal{F}_{\gamma\mathcal{S}}. \quad (4.1)$$

Consequently, the free energy of the wormhole can be minimised by minimising  $\mathcal{F}_{\mathcal{S}}$  in such a way that the consequence of the Fuchsian identifications are respected. For

instance, on the wormhole geometry the points  $P_1, P_3$  are identified with  $Q_{\mathcal{N}}$ , points  $P'_1, P'_3$  are identified with  $Q_{\mathcal{N}'}$ , points  $\tilde{P}_1, \tilde{P}_3$  are identified with  $\tilde{Q}_{\mathcal{N}}$ , points  $\tilde{P}'_1, \tilde{P}'_3$  are identified with  $\tilde{Q}_{\mathcal{N}'}$ , points  $P_2, P_4$  are identified with  $Q_{\mathcal{M}}$ , points  $P'_2, P'_4$  are identified with  $Q_{\mathcal{M}'}$ , points  $\tilde{P}_2, \tilde{P}_4$  are identified with  $\tilde{Q}_{\mathcal{M}}$ , points  $\tilde{P}'_2, \tilde{P}'_4$  are identified with  $\tilde{Q}_{\mathcal{M}'}$ .

The major contributions to the free energy  $\mathcal{F}_S$  come from the conical singularities. Therefore, the minimisation of the free energy is with respect to the locations of the conical singularities in all of the  $8n+1$  number of  $w$ -planes whose gluing give the surface  $\mathcal{S}$ . Hence, we are only required to compute the contribution from such points. From equation (3.3), it is clear that such contributions depends on the value of the angle at the conical singularity, the distance from the nearby conical singularity and the value of dilaton at the conical singularity. For example, the leading contribution to  $\mathcal{F}_S$  from the conical singularities  $P_1$  and  $P'_1$  in a  $w$ -plane that belongs to the first group is given by

$$\begin{aligned} \mathcal{F}_S^{P_1, P'_1} \approx & -\frac{n(n+1)c}{6(2n+1)} \ln(w_{P_1} - w_{P_N})(\bar{w}_{P_1} - \bar{w}_{P_N})(w_{P'_1} - w_{B_L})(\bar{w}_{P'_1} - \bar{w}_{B_L}) \\ & - \frac{n}{2(2n+1)G_N} \Phi(w_{P_1}, \bar{w}_{P_1}) - \frac{n}{2(2n+1)G_N} \Phi(w_{P'_1}, \bar{w}_{P'_1}). \end{aligned} \quad (4.2)$$

Minimising  $\mathcal{F}_S^{P_1, P'_1}$  with respect to the coordinates  $(w_{P_1}, \bar{w}_{P_1})$  of the point  $P_1$  and the coordinates  $(w_{P'_1}, \bar{w}_{P'_1})$  of the point  $P'_1$  and analytically continuing  $n$  to an infinitesimal real number determine  $P_1$  and  $P'_1$ . We can determine the locations all the other conical singularities by repeating this computation and by imposing the consequence of the Fuchsian identification by hand. We shall list the results of the free energy minimisation below.

$$\begin{aligned} (w_{P_1}, \bar{w}_{P_1}) &= (w_{\tilde{P}_1}, \bar{w}_{\tilde{P}_1}) = (w_{P_3}, \bar{w}_{P_3}) = (w_{\tilde{P}_3}, \bar{w}_{\tilde{P}_3}) \approx \left( \frac{G_N}{3} w_{P_N}, \frac{G_N}{3} \bar{w}_{P_N} \right), \\ (w_{P'_1}, \bar{w}_{P'_1}) &= (w_{\tilde{P}'_1}, \bar{w}_{\tilde{P}'_1}) = (w_{P'_3}, \bar{w}_{P'_3}) = (w_{\tilde{P}'_3}, \bar{w}_{\tilde{P}'_3}) \approx \left( \frac{G_N}{3} w_{B_L}, \frac{G_N}{3} \bar{w}_{B_L} \right) \\ (w_{P_2}, \bar{w}_{P_2}) &= (w_{\tilde{P}_2}, \bar{w}_{\tilde{P}_2}) = (w_{P_4}, \bar{w}_{P_4}) = (w_{\tilde{P}_4}, \bar{w}_{\tilde{P}_4}) \approx \left( \frac{G_N}{3} w_{B_R}, \frac{G_N}{3} \bar{w}_{B_R} \right), \\ (w_{P'_2}, \bar{w}_{P'_2}) &= (w_{\tilde{P}'_2}, \bar{w}_{\tilde{P}'_2}) = (w_{P'_4}, \bar{w}_{P'_4}) = (w_{\tilde{P}'_4}, \bar{w}_{\tilde{P}'_4}) \approx \left( \frac{G_N}{3} w_{B_L}, \frac{G_N}{3} \bar{w}_{B_L} \right). \end{aligned} \quad (4.3)$$

Notice that the location of  $P_1, \tilde{P}_1, P_3$  and  $\tilde{P}_3$  depend only on the point  $P_N$ , i.e. the distance of these points from the boundary of the gravitational region in each  $w$  plane depends only on the location of  $P_N$ . Moreover, on the wormhole surface the points  $P_1$  and  $P_3$  are identified with the point  $Q_{\mathcal{N}}$ , and the points  $\tilde{P}_1$  and  $\tilde{P}_3$  are identified with the point  $\tilde{Q}_{\mathcal{N}}$ . Therefore we can choose another slitting of the wormhole,

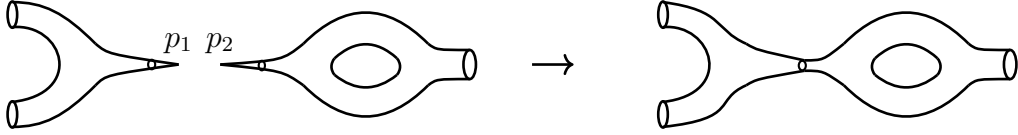


**Figure 9.** The plumbing fixture gluing of two Riemann surfaces  $\mathcal{S}_1$  and  $\mathcal{S}_2$  by identifying the neighbourhood around the punctures  $p_1$  on  $\mathcal{S}_1$  and  $p_2$  on  $\mathcal{S}_2$ .

so that the points  $P_1, \tilde{P}_1, P_3$  and  $\tilde{P}_3$  belongs to different  $w$ -planes. If we repeat the analysis we will again reach at the same conclusions. This implies that the points  $Q_{\mathcal{N}}$  and  $\tilde{Q}_{\mathcal{N}}$  must coincide on the wormhole surface. Similarly, we can argue that  $Q_{\mathcal{N}'}$  and  $\tilde{Q}_{\mathcal{N}'}$  coincide,  $Q_{\mathcal{M}}$  and  $\tilde{Q}_{\mathcal{M}}$  coincide, and  $Q_{\mathcal{M}'}$  and  $\tilde{Q}_{\mathcal{M}'}$  coincide. The net effect is that the cuts in the  $w$ -plane where the local operator  $\psi$  is inserted has become eight closely placed cuts. In which, four of the cuts have the same end points  $(\frac{G_{\mathcal{N}}}{3}w_{BL}, \frac{G_{\mathcal{N}}}{3}\bar{w}_{BL})$  and  $(\frac{G_{\mathcal{N}}}{3}w_{PN}, \frac{G_{\mathcal{N}}}{3}\bar{w}_{PN})$ . The remaining four cuts also have the same end points  $(\frac{G_{\mathcal{N}}}{3}w_{BL}, \frac{G_{\mathcal{N}}}{3}\bar{w}_{BL})$  and  $(\frac{G_{\mathcal{N}}}{3}w_{BR}, \frac{G_{\mathcal{N}}}{3}\bar{w}_{BR})$ .

Interestingly, the analysis of the CFT path integral can be simplified by considering another equivalent representation of the wormhole saddle. From the above discussion it is clear that the length of all the black coloured dotted and thick curves on the wormhole in figure 6 are infinitesimal. This suggests that all the dotted olive closed curves in figure 6 have infinitesimal lengths. Hence, we can go to an equivalent representation of the Riemann surface describing the wormhole geometry. The equivalent representation can be obtained by the plumbing fixture of another geometry  $\mathcal{R}$  with hyperbolic metric in the gravitational region. The geometry  $\mathcal{R}$  is obtained by cutting the wormhole along the olive closed curves and shrinking the olive curves to punctures. Below we shall provide a terse summary of the plumbing fixture construction. A detailed discussion of this construction can be found in [21–23].

The plumbing fixture constructs a Riemann surface by sewing two Riemann surfaces  $\mathcal{S}_1$  and  $\mathcal{S}_2$  by identifying the neighbourhood around the punctures  $p_1$  on  $\mathcal{S}_1$  and  $p_2$  on  $\mathcal{S}_2$ , see figure 9. Denote the local coordinate around the puncture  $p_1$  on  $\mathcal{S}_1$  as  $w_{p_1}$  and the local coordinate around the puncture  $p_2$  on  $\mathcal{S}_2$  as  $w_{p_2}$ . The neighbourhoods are identified using the following relation

$$w_{p_1}w_{p_2} = t, \quad 0 \leq |t| < 1, . \quad (4.4)$$

This identification removes the neighbourhood of the punctures within the cusps bounded by the curves  $w_{p_1} = \sqrt{t}$  and  $w_{p_2} = \sqrt{t}$  and sews them along the curves  $w_{p_1} = \sqrt{t}$  and  $w_{p_2} = \sqrt{t}$ , see figure 9. We shall denote the new Riemann surface produced by the sewing as  $\mathcal{S}_t$ . The hyperbolic metric around the puncture  $p_i$  in terms of the local

coordinate  $w_{p_i}$  is given by

$$ds^2 = \left( \frac{|dw_{p_i}|}{|w_{p_i}| \ln |w_{p_i}|} \right)^2 \quad i = 1, 2. \quad (4.5)$$

The neighbourhood of a puncture with this metric has no geodesics in it. Therefore, the curves  $w_{p_1} = \sqrt{t}$  and  $w_{p_2} = \sqrt{t}$  can not be geodesics. This implies that the resulting surface  $\mathcal{S}_t$  is not a hyperbolic Riemann surface. However, this metric can be made smooth and can be related to the hyperbolic metric on the surface by an appropriate Weyl rescaling [21]. The geodesic length  $l$  of the curve  $w_{p_1} = w_{p_2} = \sqrt{t}$  computed using the resulting hyperbolic metric for infinitesimal values of  $|t|$  can be approximated as

$$l = -\frac{2\pi^2}{\ln|t|}. \quad (4.6)$$

For infinitesimal values of the plumbing parameter  $|t|$ , the CFT path integral over the wormhole geometry can be approximated as the CFT path integral over  $\mathcal{R}$  obtained by shrinking the olive colored closed curves in figure 6. The surface  $\mathcal{R}$  can be constructed by gluing  $8n+1$  number of  $w$ -planes. In which, the  $4n$  number of  $w$ -planes have cuts only in the bath region, and they can be identified with  $n$  copies of the density matrices  $\rho_{\mathcal{N}'}^B$ ,  $\rho_{\mathcal{M}'}^B$ ,  $(\rho_{\mathcal{M}'}^B)^{-1}$  and  $(\rho_{\mathcal{N}'}^B)^{-1}$ . The  $4n$  number of  $w$ -planes having cuts both in the bath region and gravitational region can be identified with  $n$ -copies of the density matrices  $\rho_{\mathcal{N}^p}^{-1}$ ,  $\rho_{\mathcal{M}^p}$ ,  $\rho_{\mathcal{M}^p}^{-1}$  and  $\rho_{\mathcal{N}^p}$ . The density matrix  $\rho_{\mathcal{M}^p}$  are constructed by performing the CFT path integral over a  $w$ -plane with cut in the bath region that connects at  $B_L$  and  $\infty$ , and a cut in the gravitational region that connects the point with coordinates  $(\frac{G_N}{3}w_{B_L}, \frac{G_N}{3}\bar{w}_{B_L})$  and the point with coordinates  $(\frac{G_N}{3}w_{B_R}, \frac{G_N}{3}\bar{w}_{B_R})$ . Similarly, the density matrix  $\rho_{\mathcal{N}^p}$  can be constructed by performing the CFT path integral over a  $w$ -plane with cut in the bath region that connects at  $P_N$  and  $\infty$ , and a cut in the gravitational region that connects the point with coordinates  $(\frac{G_N}{3}w_{B_L}, \frac{G_N}{3}\bar{w}_{B_L})$  and the point with coordinates  $(\frac{G_N}{3}w_{P_N}, \frac{G_N}{3}\bar{w}_{P_N})$ . Therefore, the CFT path integral over the surface  $\mathcal{R}$  can be interpreted as the following correlation function

$$\langle \Omega | (\rho_{\mathcal{N}'}^B)^n \otimes \rho_{\mathcal{N}^p}^{-n} (\rho_{\mathcal{M}'}^B)^{-n} \otimes \rho_{\mathcal{M}^p}^n \psi(w_P, \bar{w}_P) \rho_{\mathcal{M}^p}^{-n} \otimes (\rho_{\mathcal{M}'}^B)^n \rho_{\mathcal{N}^p}^n \otimes (\rho_{\mathcal{N}'}^B)^{-n} | \Omega \rangle.$$

From this, we can infer that the wormhole saddle extends the operator algebra  $\mathcal{N}$  to  $\mathcal{N}_p$  and  $\mathcal{M}$  to  $\mathcal{M}_p$ . The extended operator algebra  $\mathcal{N}_p$  is the union of operator algebra  $\mathcal{N}$  and the operator algebra in the domain of dependence of the interval whose end points are  $(\frac{G_N}{3}w_{B_L}^+, \frac{G_N}{3}w_{B_L}^-)$  and  $(\frac{G_N}{3}w_{P_N}^+, \frac{G_N}{3}w_{P_N}^-)$ . Likewise, the extended operator algebra  $\mathcal{M}_p$  is the union of operator algebra  $\mathcal{M}$  and the operator algebra in the domain of dependence of the interval whose end points are  $(\frac{G_N}{3}w_{B_L}^+, \frac{G_N}{3}w_{B_L}^-)$  and  $(\frac{G_N}{3}w_{B_R}^+, \frac{G_N}{3}w_{B_R}^-)$ .

### 4.3 The modular flow for a free chiral scalar in two intervals

The action of the half-sided translations associated with the extended algebras  $\mathcal{M}_p$  and  $\mathcal{N}_p$  can be understood by studying the transformation generated by  $\Delta_{\mathcal{M}_p}$  and  $\Delta_{\mathcal{N}_p}$ , the modular operators for the operator algebras  $\mathcal{M}_p$  and  $\mathcal{N}_p$  respectively. Unfortunately, the modular operator associated with two intervals for an interacting CFT is not known. However, this is known for the special case described below.

Consider the algebra  $\mathcal{A}$  of a current  $j(w^-) = \partial_{w^-} \psi(w^-)$  in a free massless scalar field  $\psi$  in 2 dimension for a two interval region  $A = A_1 \cup A_2$  on the  $w^-$  line. The interval  $A_1$  is given by  $a_1 < w^- < b_1$ , and the interval  $A_2$  is given by  $a_2 < w^- < b_2$ . Let us describe the modular evolution of the operator linear in the current

$$\mathcal{O} = \int_A dw^- \gamma(w^-) j(w^-),$$

where  $\gamma(w^-)$  is an arbitrary distribution. It is an element of the operator algebra  $\mathcal{A}$ . The function  $\gamma(w^-)$  can be decomposed in terms of the eigenvectors  $u_{k,s}(w^-)$ ,  $k = 1, 2, s \in \mathbb{R}$ , of the modular Hamiltonian kernel [24] as follows

$$\gamma(w^-) = \sum_{k=1}^2 \int_{-\infty}^{\infty} ds c_k(s) u_{k,s}(w^-). \quad (4.7)$$

Then the modular flow of the operator  $\mathcal{O}$  can be conveniently described as follows

$$\mathcal{O}_t = \Delta_{\mathcal{A}}^{-it} \mathcal{O} \Delta_{\mathcal{A}}^{it} = \sum_{k=1}^2 \int_A dw^- \int_{-\infty}^{\infty} ds e^{2\pi i s t} c_k(s) u_{k,s}(w^-). \quad (4.8)$$

Assume that the operator  $\mathcal{O}(w_0^-)$  is localised at a point  $w_0^-$  that belongs to the interval  $A_2$ . It can be obtained by choosing  $\gamma(w^-)$  to be the Dirac delta function  $\delta(w^- - w_0^-)$ . The Dirac delta function can be decomposed in terms of the eigenvectors  $u_{k,s}(w^-)$  as follows

$$\delta(w^- - w_0^-) = 2 \frac{dh(w^-)}{dw^-} \int_{-\infty}^{\infty} ds |s| u_{1,s}^*(w_0^-) u_{1,s}(w^-) \quad (4.9)$$

where

$$h(x) = \ln \left( \frac{(x - a_1)(x - a_2)}{(x - b_1)(x - b_2)} \right)$$

and  $u_{1,s}(x) = \frac{1}{\sqrt{4\pi|s|}} e^{-ih(x)}$ . From this, we can identify the coefficient  $c_k(s)$  for the delta function

$$c_k(s) = 2\delta_{k,1} \frac{dh(w^-)}{dw^-} |s| u_{1,s}^*(w_0^-). \quad (4.10)$$

Therefore, the modular flowed operator  $\mathcal{O}_t(w_0^-)$  is given by

$$\mathcal{O}_t(w_0^-) = \int_A dw^- \int_{-\infty}^{\infty} ds e^{2\pi i s t} c_1(s) u_{1,s}(w^-) = \sum_q \mathcal{O}(w_q^-(t)) + \sum_q \mathcal{O}(\tilde{w}_q^-(t)), \quad (4.11)$$

where  $\{w_q^-(t), \tilde{w}_q^-(t)\}$  are solutions of the following algebraic equation

$$h(w^-(t)) = h(w_0^-) - 2\pi t. \quad (4.12)$$

The solutions  $\{w_q^-(t)\}$  belong to the interval  $A_2$  and the solutions  $\{\tilde{w}_q^-(t)\}$  belong to the interval  $A_1$ . This shows that the action of the modular operator  $\Delta_{\mathcal{A}}$  on a local operator localised in the interval  $A_2$  spread it into the disconnected interval  $A_1$ .

#### 4.4 The action of the reduced half-sided translations after the Page time

The action of the reduced half-sided translations on the local operator  $\mathcal{O}(w_P^-)$  in the extended operator algebra  $\mathcal{N}_p$  localised at a point  $P$  in the bath region with  $w^- = w_0^-$  after the Page time is given by

$$\mathcal{O}^s(w_P^-) = \Delta_{\mathcal{N}_p}^{-it} \Delta_{\mathcal{M}_p}^{it} \mathcal{O}(w_P^-) \Delta_{\mathcal{M}_p}^{-it} \Delta_{\mathcal{N}_p}^{it} = \sum_r \mathcal{O}(w_r^-) + \sum_r \mathcal{O}(\tilde{w}_r^-), \quad (4.13)$$

where  $s = e^{-2\pi i t} - 1$  and  $\{w_r^-(t), \tilde{w}_r^-(t)\}$  are solutions of the following algebraic equation

$$h_{\mathcal{N}_p}(w^-(t)) = h_{\mathcal{N}_p}(h_{\mathcal{M}_p}^{-1}(h_{\mathcal{M}_p}(w_0^-) - 2\pi t)) + 2\pi t, \quad (4.14)$$

where

$$h_{\mathcal{N}_p}(w^-) = \ln \left( \frac{(w^- - w_{B_L}^-)(w^- - w_{B_R}^-)}{(w^- - \frac{G_N}{3} w_{P_N}^-)} \right)$$

and

$$h_{\mathcal{M}_p}(w^-) = \ln \left( \frac{(w^- - w_{B_L}^-)(w^- - w_{B_R}^-)}{(w^- - \frac{G_N}{3} w_{B_R}^-)} \right).$$

The solutions  $\{w_r^-(t)\}$  belong to the island and the solutions  $\{\tilde{w}_r^-(t)\}$  belong to the bath. This proves that the reduced half-sided translations after the Page time converts a local operator localised in the bath region into a non-local operator that spread into the island. Hence, we conclude that after the Page time bath degrees of freedom reconstruct the operators in the interior of the black hole. This is in perfect agreement with the second assertion of the island paradigm, which states that after the Page time the operators in the black hole interior can be reconstructed using the operators in the bath.

## 5 Conclusion

In this paper, we demonstrated that the island paradigm by describing a procedure to express the degrees of freedom inside the black hole interior using only the degrees of freedom in the bath using the notion of the reduced half-sided translations. It will be interesting to investigate how this procedure is realised if the matter CFT has a dual three dimensional gravitational description.

## Acknowledgements

We are grateful to Sujay Ashok and Alok Laddha for the numerous discussions and comments. We also thank Horacio Casini for a helpful clarification.

## References

- [1] K. Jalan and R. Pius, *Half-sided Translations and Islands*, [2312.11085](#).
- [2] S.W. Hawking, *Breakdown of Predictability in Gravitational Collapse*, *Phys. Rev. D* **14** (1976) 2460.
- [3] S.W. Hawking, *Particle Creation by Black Holes*, *Commun. Math. Phys.* **43** (1975) 199.
- [4] D.N. Page, *Average entropy of a subsystem*, *Phys. Rev. Lett.* **71** (1993) 1291 [[gr-qc/9305007](#)].
- [5] A. Almheiri, R. Mahajan, J. Maldacena and Y. Zhao, *The Page curve of Hawking radiation from semiclassical geometry*, *JHEP* **03** (2020) 149 [[1908.10996](#)].
- [6] A. Almheiri, T. Hartman, J. Maldacena, E. Shaghoulian and A. Tajdini, *The entropy of Hawking radiation*, *Rev. Mod. Phys.* **93** (2021) 035002 [[2006.06872](#)].
- [7] A. Almheiri, R. Mahajan and J. Maldacena, *Islands outside the horizon*, [1910.11077](#).
- [8] K. Papadodimas and S. Raju, *Local Operators in the Eternal Black Hole*, *Phys. Rev. Lett.* **115** (2015) 211601 [[1502.06692](#)].
- [9] S. Leutheusser and H. Liu, *Causal connectability between quantum systems and the black hole interior in holographic duality*, [2110.05497](#).
- [10] S. Leutheusser and H. Liu, *Emergent times in holographic duality*, [2112.12156](#).
- [11] H.J. Borchers, *On revolutionizing quantum field theory with Tomita's modular theory*, *J. Math. Phys.* **41** (2000) 3604.
- [12] P. Calabrese and J.L. Cardy, *Entanglement entropy and quantum field theory*, *J. Stat. Mech.* **0406** (2004) P06002 [[hep-th/0405152](#)].

- [13] A. Almheiri, T. Hartman, J. Maldacena, E. Shaghoulian and A. Tajdini, *Replica Wormholes and the Entropy of Hawking Radiation*, *JHEP* **05** (2020) 013 [[1911.12333](#)].
- [14] E. Witten, *APS Medal for Exceptional Achievement in Research: Invited article on entanglement properties of quantum field theory*, *Rev. Mod. Phys.* **90** (2018) 045003 [[1803.04993](#)].
- [15] S. Hollands, *On the modular operator of mutli-component regions in chiral CFT*, *Commun. Math. Phys.* **384** (2021) 785 [[1904.08201](#)].
- [16] A. Lewkowycz and J. Maldacena, *Generalized gravitational entropy*, *JHEP* **08** (2013) 090 [[1304.4926](#)].
- [17] J.L. Cardy and I. Peschel, *Finite Size Dependence of the Free Energy in Two-dimensional Critical Systems*, *Nucl. Phys. B* **300** (1988) 377.
- [18] T. Jacobson, *Entanglement Equilibrium and the Einstein Equation*, *Phys. Rev. Lett.* **116** (2016) 201101 [[1505.04753](#)].
- [19] Y. Iwayoshi and M. Taniguchi, *An introduction to Teichmüller spaces*, Springer Science & Business Media (2012).
- [20] H. Pan, *On finite marked length spectral rigidity of hyperbolic cone surfaces and the thurston metric*, 2017.
- [21] K. Obitsu and S.A. Wolpert, *Grafting hyperbolic metrics and eisenstein series*, *Mathematische Annalen* **341** (2008) 685.
- [22] S.F. Moosavian and R. Pius, *Hyperbolic geometry and closed bosonic string field theory. Part I. The string vertices via hyperbolic Riemann surfaces*, *JHEP* **08** (2019) 157 [[1706.07366](#)].
- [23] S.F. Moosavian and R. Pius, *Off-Shell Amplitudes in String Theory and Hyperbolic Geometry*, *Fortsch. Phys.* **68** (2020) 1900078 [[1703.10563](#)].
- [24] R.E. Arias, H. Casini, M. Huerta and D. Pontello, *Entropy and modular Hamiltonian for a free chiral scalar in two intervals*, *Phys. Rev. D* **98** (2018) 125008 [[1809.00026](#)].